Enhanced Energy Prediction of Next-Generation Urban Buildings Optimized with Pyramidal Dilation Attention Convolutional Deep Neural Networks

Suleman Alnatheer
Department of Computer Engineering, College of Computer Engineering & Sciences, Prince Sattam bin Abdulaziz University, Alkharj, Saudi Arabia
s.alnatheer@psau.edu.sa (corresponding author)

Mohammed Altaf Ahmed
Department of Computer Engineering, College of Computer Engineering & Sciences, Prince Sattam bin Abdulaziz University, Alkharj, Saudi Arabia
m.altaf@psau.edu.sa

Received: 1 July 2025 | Revised: 9 August 2025 | Accepted: 20 August 2025

 DOI: https://doi.org/10.48084/etasr.13097

ABSTRACT

Investors, urban designers, and energy policymakers increasingly rely on modeling and analysis of building energy performance to develop long-term sustainable energy strategies that reduce energy consumption and emissions. However, a gap remains between building energy modeling and conventional planning techniques due to inconsistent energy data and the lack of scalable building models. In this work, we propose the Enhanced Energy Prediction of Next-Generation Urban Buildings Optimized with Pyramidal Dilation Attention Convolutional Deep Neural Network and Bitterling Fish Optimization (EEP-UB-PDACN-BFO). The approach begins with input data obtained from the Building Energy Ratings (BER) dataset, which is preprocessed using the Bilinear Double-Order Filter (BDOF) to detect and remove inconsistencies. The preprocessed data are then passed through the Pyramidal Dilation Attention Convolutional Network (PDACN) to forecast the Energy Use Intensity (EUI) of buildings. To further improve accuracy, Bitterling Fish Optimization (BFO) is applied to optimize the weight parameters of the PDACN. The proposed EEP-UB-PDACN-BFO model is implemented in Python and evaluated using performance metrics including Root Mean Square Error (RMSE), Mean Absolute Error (MAE), Mean Absolute Percentage Error (MAPE), Mean Square Error (MSE), and the coefficient of determination (R^2). The proposed method achieves an R^2 of 0.95, an RMSE of 6.2 kWh/(m^2·year), and an MAE of 3.9 kWh/(m^2·year), outperforming existing approaches. These results demonstrate that the proposed method substantially enhances building performance modelling, providing a more robust tool for the development of sustainable energy policies and industrial regulations.

Keywords-energy performance; sustainable energy and industry; building energy rating dataset; urban building; residential building; environment; building energy; smart cities

I. INTRODUCTION

In 2021, building activities accounted for 27% of total Greenhouse Gas (GHG) emissions from the energy sector and 30% of global energy consumption. Of these emissions, 8% were direct, occurring within the buildings themselves, while 19% were indirect, originating from energy and heat produced and consumed inside the buildings [1-3]. In response, the Energy Performance of Buildings Directive (EPBD) was enacted by EU member states to strengthen energy efficiency in the construction industry and support sustainable strategic planning [4, 5]. The directive aims to accelerate the adoption of energy efficiency policies so that by 2030 and 2050, the building stock will be highly energy-efficient and decarbonized.

With rising annual energy consumption, particularly in urban areas, carbon emissions are projected to increase significantly. Consequently, reducing energy use and emissions from the building sector has become increasingly urgent. Urban planners and policymakers are therefore investigating comprehensive sustainable energy plans to retrofit existing structures and improve their sustainability [6-9]. Long-term rehabilitation strategies are also required to enhance sustainability and reduce emissions, supported by rigorous analysis of building energy performance data. However, the development of efficient and durable energy conservation solutions is often hindered by limited access to reliable datasets, creating challenges for manufacturers, utility planners, urban designers, and policymakers. The scarcity of complete and scalable urban data hampers an accurate understanding of city-wide energy systems [10-12].

Two principal approaches are used for building energy performance analysis: physical models and data-driven models [13]. Physical modeling tools, such as Transient System Simulation Tool (TRNSYS), EnergyPlus, and ESP-r, are grounded in detailed construction physics, requiring extensive geometric and non-geometric architectural data [14-16]. In contrast, data-driven methods employ statistical and machine learning techniques, including Gradient Boosting (GB), Artificial Neural Networks (ANNs), and Graph Convolutional Networks (GCNs), to predict energy consumption from historical data, without necessitating full architectural specifications [17-20]. While effective, these approaches face challenges such as overfitting (GB), vanishing gradients and large dataset requirements (ANNs), and scalability issues or over-smoothing in large graphs (GCNs).

Urban-scale applications further amplify these difficulties, as time-series forecasting must adapt to dynamic systems, while trade-offs between energy efficiency and indoor comfort introduce computational complexity. Remote sensing, imagery, and smart meter data add value but often suffer from limited resolution and socio-economic heterogeneity. Large-scale assessments can also over-generalize outcomes, failing to capture the nuanced diversity of urban environments. For instance, studies such as those targeting Smart City Thailand highlight the need for improved models to enhance energy efficiency and reduce GHG emissions [21].

To address these limitations, this paper proposes the Enhanced Energy Prediction of Next-Generation Urban Buildings Optimized with Pyramidal Dilation Attention Convolutional Network and Bitterling Fish Optimization (EEP-UB-PDACN-BFO). The method integrates the Building Energy Ratings (BER) dataset, employs the Bilinear Double-Order Filter (BDOF) for data preprocessing, and applies the Pyramidal Dilation Attention Convolutional Network (PDACN) for accurate prediction of Energy Use Intensity (EUI). To further improve robustness, BFO is used to optimize the PDACN weight parameters. The effectiveness of this hybrid framework is validated through comprehensive performance metrics, demonstrating substantial improvements in prediction accuracy and scalability for urban building energy modeling.

II. MATERIALS AND METHODS

In this study, supervised PDACN is applied to forecast large-scale building energy performance. By combining data-driven methodologies with physics-based insights, the approach seeks to identify the most efficient prediction model. As illustrated in Figure 1, the forecasting process for urban building energy performance involves five sequential stages.

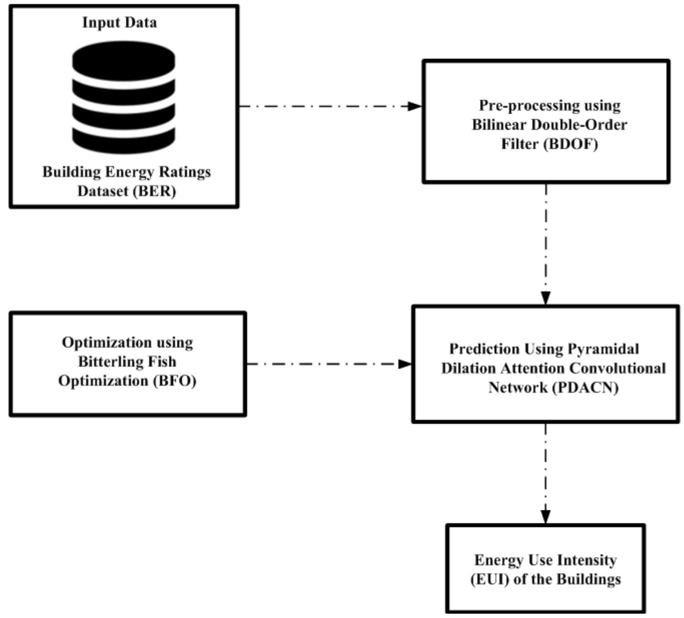

Fig. 1. Block diagram for the proposed EEP-UB-PDACN-BFO method.

A. *Data Acquisition*

The Irish BER dataset is a comprehensive compilation of energy efficiency evaluations conducted on residential and commercial buildings in Ireland [22]. The dataset is sourced from the National BER Register, managed by the Sustainable Energy Authority of Ireland (SEAI). It includes a diverse range of building types, such as single-family homes, apartments, offices, retail establishments, and other non-domestic structures, covering both new constructions and existing buildings. Key dataset characteristics include BER, building attributes (location, floor area, number of floors, construction year, and architectural features), energy performance indicators (primary energy consumption, CO_2 emissions, heating and cooling demand), and information on renewable energy features such as solar panels, wind turbines, and heat pumps. The dataset provides building-level granularity and temporal coverage over multiple years, enabling detailed analysis of energy efficiency trends, benchmarking, and modelling.

B. *Preprocessing Using Bilinear Double-Order Filter (BDOF)*

The BDOF [23] is employed in the preprocessing stage with the primary role of identifying and eliminating inconsistencies in the dataset, thereby improving data quality and reliability. BDOF's ability to adjust to specific energy consumption patterns makes it suitable for large-scale urban applications. By accurately estimating energy use, BDOF supports building owners and operators in optimizing energy management strategies, improving efficiency, and reducing costs.

BDOF's extraordinary sensitivity to long-term climatic fluctuations is mathematically expressed in the following equations.

$$J_{DO}(u) = I_N \cdot \left[\frac{\alpha(\tau u)^{\alpha}+1}{z(\tau u)^{\alpha}+1}\right]^{\beta} \quad (1)$$

where J_{DO} represent the filtered values, I_N represent the input data in a suitable range for the filter, τ is the discrete or continuous input variable, $z(tu)$ is the zero polynomial term, $a(\tau u)$ is the pole polynomial term, α and β are the nonlinearity and sensitivity exponents. Equation (1) provides the poles and zeros of the filters, so (2) can be used to generate the transfer function for the linguistic process:

$$J_{DO}(u) = I_N \cdot \left(\frac{\omega_r}{\omega_b}\right)^{\alpha\beta} \left[\frac{u^\alpha + \omega_b^\alpha}{u^\alpha + \omega_r^\alpha}\right]^\beta \quad (2)$$

where, u denotes the output data, and I_N represent the gain at the upper data level. Equation (3) illustrates the resulting normalization of the data for urban building, which has the form necessary to achieve the programmability of the BDOF functions.

$$J_{app}(u) \approx \frac{F_3u^3+F_2u^2+F_1u+F_0}{u^3+E_2u^2+E_1u+E_0} \quad (3)$$

where J_{app} represent the normalized filter output, E_0, E_1, and E_2 are denominator coefficients, F_0, F_1, F_2, F_3 are numerator coefficients. The feedback structure of BDOF can be implemented as:

$$E_{FLF}(u) = \frac{I_3u^3+\frac{I_2}{\tau_1}u^2+\frac{I_1}{\tau_1\tau_2}u+\frac{I_0}{\tau_1\tau_2\tau_3}}{u^3+\frac{1}{\tau_1}u^2+\frac{1}{\tau_1\tau_2 u}+\frac{1}{\tau_1\tau_2\tau_3}} \quad (4)$$

where E_{FLF} represent the BDOF applied to the input, τ_1, τ_2, τ_3 denotes the feedback coefficients; and I_0, I_1, I_2, I_3 represent the denominator coefficients. Through these operations, BDOF ensures that only consistent, high-quality data is passed forward to the prediction stage.

C. Prediction Using Pyramidal Dilation Attention Convolutional Network (PDACN)

The PDACN [24] is utilized to predict the EUI of buildings. Its primary goal is to capture multi-scale contextual features and complex spatial dependencies within building energy data by combining pyramidal dilation with attention mechanisms. This enables the model to emphasize relevant patterns while preserving spatial hierarchies, thereby producing more robust and reliable predictions. PDACN enhances the representational capacity of deep networks, making it highly suitable for heterogeneous and high-dimensional urban energy datasets, ultimately supporting informed energy management and planning decisions. The approach also facilitates anticipatory actions for building safety, emergency response, and mitigation of infrastructure and public health impacts. The mathematical formulation of PDACN includes multi-scale feature aggregation (5), attention-based scaling (6), attention score computation (7), a combined loss function (8), and margin computation for classification confidence (9). The multi-scale feature aggregation is performed using:

$$M_k = n_1^1 \wedge n_2^2 \wedge n_3^4 \wedge \dots n_d^k \quad (5)$$

where M_k denotes the combined multi-scale feature map or aggregated representation at the k^{th} level, n_1^1 represent the individual features at different levels of the network, n_d^k is the dilation scale or hierarchical contribution of each feature, and $\wedge$ denotes the logical combination or feature fusion between layers. The attention-based scaling is performed using:

$$g_k' = H_{scale}(g_k, s_k) = s_k \cdot g_k, k = 1, \dots b \quad (6)$$

where g_k represent the feature map or representation at the layer k, s_k represent the scaling or attention factor for the layer k, H_{scale} is the function that scales the feature map, and g_k' is the output feature map after applying the attention-based scaling. The attention score computation is calculated using:

$$s\alpha = sigm([s\alpha^{avg}, s\alpha^{max}] * E) \quad (7)$$

where $*$ represent the quantity of energy used per m^2, $s\alpha$ represent the attention score or weight for a specific channel or feature, $sigm$ is the Sigmoid activation function to normalize the attention score between 0 and 1, $s\alpha^{avg}$ is the average-pooled representation of the feature map, $s\alpha^{max}$ is the max-pooled representation of the feature map, and E is the weight matrix. The combined loss function is calculated using:

$$l_{sce} = \alpha l_{ce} + (1-\alpha) l_{rce} \quad (8)$$

where, l_{sce} is the combined loss function used to train PDACN, l_{ce} is the standard cross-entropy loss for regression, l_{rce} is the reverse cross-entropy loss, often used to handle noisy labels, α is the weighting factor between 0 and 1, balancing the contribution of $l_{ce}$and l_{rce}. Lastly, the margin computation for classification confidence is calculated using:

$$BvSB(z_i) = P_B(z_i) - P_{SB}(z_i) \quad (9)$$

where $BvSB(z_i)$ is the margin for the i^{th} data sample z_i, $P_B(z_i)$ is the probability of the predicted best class for the sample z_i, and $P_{SB}(z_i)$ is the probability of the second-best predicted class for the sample z_i.

D. Optimization Using Bitterling Fish Optimization (BFO)

The BFO [25] algorithm is employed to optimize the weight parameters αl_{ce} and $P_B(z_i)$ in the PDACN framework, thereby enhancing the prediction accuracy of EUI in buildings. BFO offers distinct advantages, including a strong balance between exploration and exploitation, efficient avoidance of local minima, and adaptive search behaviour inspired by natural fish foraging.

Compared to other optimization algorithms such as Particle Swarm Optimization (PSO) or Genetic Algorithms (GA), BFO demonstrates faster convergence and improved stability in reaching global optima. The BFO optimization includes several steps.

1) Step 1: Initialization Phase

In the initialization phase, the BFO algorithm begins by defining the search space for the PDACN network parameters, such as weights and biases. Initial positions of the "bitterling fish" population are generated randomly within the defined boundaries.

$$H = \begin{bmatrix} H_1^1 & H_1^2 & \dots & H_1^C \\ H_2^1 & H_2^2 & \dots & H_2^C \\ \dots & \dots & \dots & \dots \\ H_n^1 & H_n^2 & \dots & H_n^C \end{bmatrix} \quad (10)$$

where C the number of dimensions in the search space, and H represents the initial population matrix of size $n \times C$.

2) Step 2: Random Generation

Input elements are generated randomly, and the best fitness values are selected under a defined hyper-parameter condition.

3) Step 3: Fitness Function

A candidate solution is generated and evaluated using the fitness function:

$$Fitnessfunction = [\alpha l_{ce}, P_B(z_i)] \tag{11}$$

where αl_{ce} aims to maximize the coefficient of determination R^2, and $P_B(z_i)$ aims to minimize Root Mean Square Error (RMSE).

4) Step 4: Escape and not Seize the Oyster for Optimizing αl_{ce}

This step mimics bitterling fish avoiding unproductive regions. Fish encountering poor fitness values move away, preventing stagnation in suboptimal areas and ensuring exploration of more promising network parameter configurations, as represented by (12):

$$\alpha l_{ce} = \begin{cases} K.F_i^t + (F * -K.N).\zeta r \leq 0.5 \\ l + (u - l).\zeta r > 0.5 \end{cases} \tag{12}$$

where $K.F_i^t$ denotes the current fitness of the candidate, $F *$ denotes the global best fitness, $K.N$ is the neighborhood fitness, ζ is the random variable controlling stochastic exploration, and u is the scaling factor affecting the influence of neighborhood exploration.

5) Step 5: Hunting Fish for Optimizing $P_B(z_i)$

In this phase, fish move toward positions with higher fitness values, refining promising network parameters. These collective movements help the PDACN converge to an optimal set of weights and biases, which can be identified using:

$$P_B(z_i) = \frac{f(F_j^t)}{\sum_{i=1}^{n} k_{ij}} \tag{13}$$

where k_{ij} is the weight factor or influence coefficient for the neighbor j on fish i, and $f(F_j^t)$ is the fitness value of fish j at time t.

6) Step 6: Termination Criteria

The optimization process repeats Steps 3-5 until a stopping criterion is met ($H = H + 1$). The result is a set of optimized PDACN parameters that improve prediction accuracy, yielding higher R^2 and lower RMSE. The complete optimization workflow of EEP-UB-PDACN-BFO is illustrated in Figure 2.

E. Experimental Evaluation

The proposed approach was implemented in Python and tested on a system with an Intel® Core™ i3-3220 Central Processing Unit (CPU) (3.30 GHz), 4 GB Random Access Memory (RAM), and a 64-bit Windows Operating System (OS). The dataset was split into 80% training and 20% testing subsets. Performance metrics, including RMSE, Mean Absolute Error (MAE), Mean Squared Error (MSE), Mean Absolute Percentage Error (MAPE), and R^2, were used for evaluation.

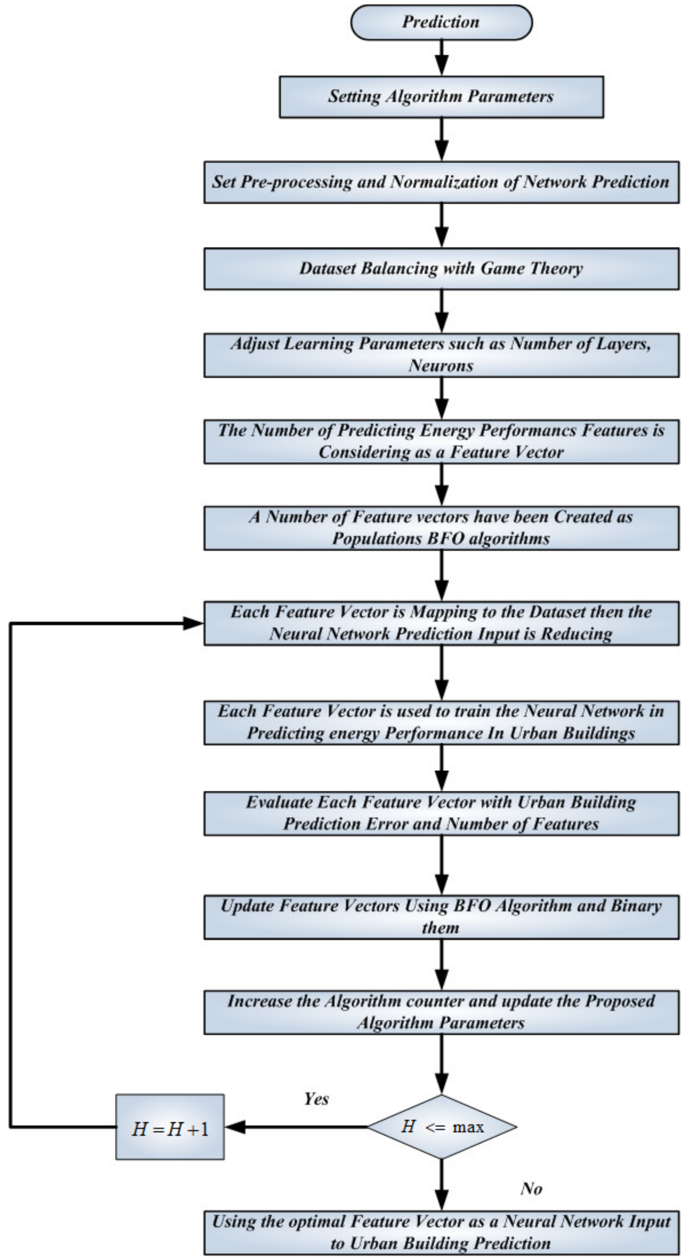

Fig. 2. Flow chart for EEP-UB-PDACN-BFO.

1) Root Mean Square Error (RMSE)

RMSE quantifies the differences between predicted and observed values by computing the square root of the mean squared residuals. It is widely used in supervised learning due to its sensitivity to large errors:

$$RMSE = \sqrt{\frac{\sum_{i=1}^{N} ||y(i) - \hat{y}(i)||^2}{n}} \tag{14}$$

where $y(i)$ and $\hat{y}(i)$ denote observed and predicted values, respectively, and n is the number of observations.

2) *Mean Absolute Error (MAE)*

MAE measures the average magnitude of prediction errors without considering their direction, providing a straightforward interpretation of model accuracy:

$$MAE = \frac{\sum_{i=1}^{n} |y_i - x_i|}{n} \quad (15)$$

where y_i is denoted as the prediction, n is indicated as the total number of data points, and x_i is denoted as the true value.

3) *Coefficient of Determination (R^2)*

R^2 indicates the proportion of variance in the dependent variable that is predictable from the independent variable:

$$R^2 = 1 - \frac{RSS}{TSS} \quad (16)$$

where RSS is the residual sum of squares and TSS is the total sum of squares.

4) *Mean Squared Error (MSE)*

MSE calculates the average squared differences between predicted and observed values, emphasizing larger errors:

$$MSE = \frac{1}{n} + \sum_{i=1}^{n} (yi - \hat{y}i) \quad (17)$$

5) *Mean Absolute Percentage Error (MAPE)*

MAPE expresses prediction accuracy as a percentage of the error relative to actual values:

$$MAPE = \frac{100\%}{n} \sum_{i=1}^{n} \left| \frac{yi - \hat{y}i}{yi} \right| \quad (18)$$

F. *Benchmarking Against Existing Methods*

The performance of the proposed EEP-UB-PDACN-BFO approach was benchmarked using the BER dataset against the Gradient Boosting Algorithm (UBEPP-RAD-GBA) [26], the Time Series Forecasting for Urban Building Energy Consumption according to Graph Convolutional Network (TSF-UBEC-DCN) [27], and the Multi-objective Optimization of Building Energy Performance and Indoor Thermal Comfort by Combining Artificial Neural Networks and Metaheuristic Algorithms (BEP-ITC-ANN) [28].

III. RESULTS

A. *Performance Analysis*

Figure 3 presents the comparative analysis of RMSE across different energy prediction methods for next-generation urban buildings. The proposed EEP-UB-PDACN-BFO method achieved the lowest RMSE of 6.2 kWh/(m^2·year). In comparison, the TSF-UBEC-GCN and BEP-ITC-ANN methods yielded higher RMSE values of 9.3 kWh/(m^2·year) and 8.4 kWh/(m^2·year), respectively, while UBEPP-RAD-GBA achieved an intermediate RMSE of 7.1 kWh/(m^2·year).

Figure 4 illustrates the distribution of synthetic residential buildings across Irish BER energy performance labels, ranging from A1 (most energy-efficient) to G (least energy-efficient). The distribution shows that the majority of buildings are concentrated in the mid-range categories, with B2 and B3 ratings being most frequent (counts of 730 and 800, respectively). In comparison, very few buildings are classified under the highest efficiency rating A1 or the lowest categories F and G, indicating that extremely efficient or inefficient buildings are underrepresented. This distribution suggests that most of the synthetic buildings exhibit moderate energy performance in terms of EUI and associated CO_2 emissions, aligning with typical patterns observed in real residential building datasets.

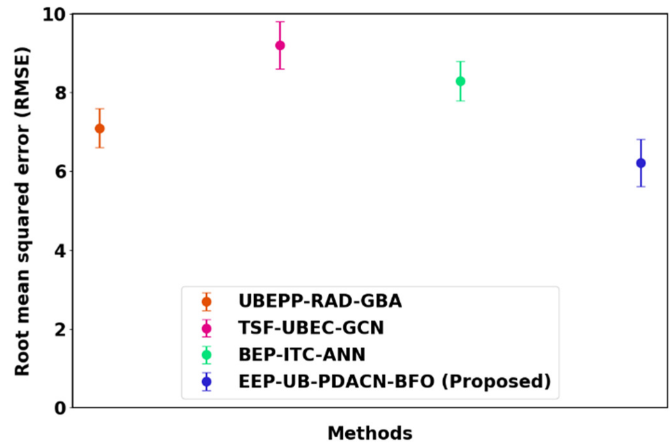

Fig. 3. Performance analysis using RMSE.

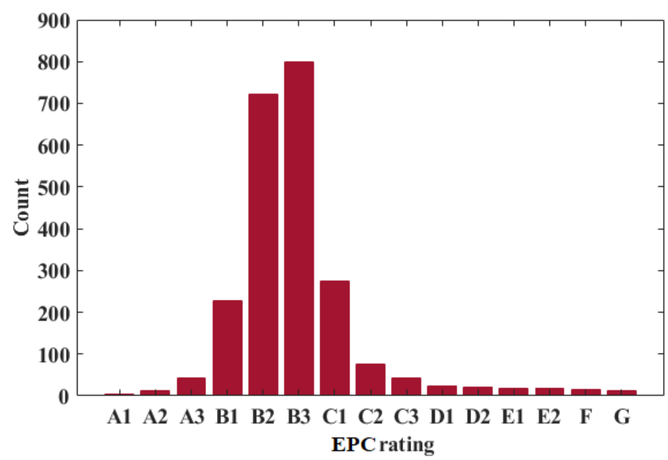

Fig. 4. Analysis of synthetic residential building data using Irish BER labels.

Table I presents the performance analysis based on the R^2. The proposed method attained the highest R^2 value of 0.95, indicating excellent predictive accuracy and a strong fit between the predicted and actual energy consumption data. In contrast, the UBEPP-RAD-GBA, TSF-UBEC-GCN, and BEP-ITC-ANN methods attained lower R^2 values of 0.5, 0.8, and 0.6, respectively, reflecting comparatively weaker performance.

Table II presents the comparative performance analysis based on the MAE metric. The proposed model achieved the lowest MAE of 3.9 kWh/(m^2·year), indicating a significantly higher prediction accuracy and lower error in estimating energy consumption in next-generation urban buildings. In comparison, the UBEPP-RAD-GBA, TSF-UBEC-GCN, and BEP-ITC-ANN methods reported higher MAE values of 5.3

kWh/(m^2·year), 8.5 kWh/(m^2·year), and 6.5 kWh/(m^2·year), respectively.

Table III compares the performance of the proposed method across different datasets using RMSE, MAE, and R^2. The proposed BER dataset showed the best results, with the lowest RMSE of 6.2 kWh/(m^2·year), MAE of 3.9 kWh/(m^2·year), and the highest R^2 of 0.95. In comparison, the Irish BER database, real-time electricity consumption data, and Energy Management Information System (EMIS) database showed slightly higher RMSE and MAE values, along with lower R^2 scores.

TABLE I. PERFORMANCE ANALYSIS OF R^2 COMPARED WITH PROPOSED AND EXISTING TECHNIQUES

Methods	R^2
EEP-UB-PDACN-BFO (Proposed)	0.95
UBEPP-RAD-GBA	0.5
TSF-UBEC-GCN	0.8
BEP-ITC-ANN	0.6

TABLE II. PERFORMANCE ANALYSIS OF MAE COMPARED WITH PROPOSED AND EXISTING TECHNIQUES

Methods	MAE (kWh/(m^2·year))
EEP-UB-PDACN-BFO (Proposed)	3.9
UBEPP-RAD-GBA	5.3
TSF-UBEC-GCN	8.5
BEP-ITC-ANN	6.5

TABLE III. ANALYSIS OF THE PROPOSED METHOD WITH DIFFERENT DATASETS

Dataset	RMSE (kWh/(m^2·year))	MAE (kWh/(m^2·year))	R^2
Irish BER Database [4]	6.48	4.25	0.91
Real-time electricity consumption data [26]	7.6	5.3	0.89
EMIS Database [27]	6.9	4.8	0.93
BER (Proposed)	6.2	3.9	0.95

Table IV compares the proposed EEP-UB-PDACN-BFO method with existing energy prediction techniques for next-generation urban buildings using MSE and MAPE metrics. The proposed method achieved the lowest MSE of 0.0750 √(kWh/(m^2·year)) and MAPE of 0.45%, indicating the highest prediction accuracy. In contrast, UBEPP-RAD-GBA and TSF-UBEC-GCN achieved much higher errors, with MSE values of 9 √(kWh/(m^2·year)) and MAPE above 27%. BEP-ITC-ANN performed closer to the proposed method but still had higher errors with an MSE of 0.0829 √(kWh/(m^2·year)) and MAPE of 0.50%.

TABLE IV. ANALYSIS OF THE PROPOSED METHOD WITH EXISTING METHODS

Methods	MSE √(kWh/(m^2·year))	MAPE (%)
EEP-UB-PDACN-BFO (Proposed)	0.0750	0.45
UBEPP-RAD-GBA	9.1734	36.34167
TSF-UBEC-GCN	9.146	27.28
BEP-ITC-ANN	0.0829	0.50

IV. DISCUSSION

The proposed EEP-UB-PDACN-BFO framework effectively addresses critical challenges in urban energy modelling by enabling accurate prediction of EUI and overcoming limitations of inconsistent energy data and poor scalability in conventional approaches. By employing BDOF for robust data preprocessing and optimizing PDACN with BFO, the method significantly improves predictive performance. Comparative evaluation demonstrates reductions in MAE and RMSE, along with a higher R^2 value compared to existing techniques, confirming the proposed model's superior accuracy, reliability, and robustness in minimizing prediction errors and enhancing urban energy forecasting.

Furthermore, the BER label distribution analysis confirms the realism of the synthetic dataset, with most buildings concentrated in the B2 and B3 efficiency categories, consistent with patterns observed in real residential datasets. Overall, these findings validate the practical relevance of the proposed framework for accurate energy prediction and informed urban energy planning.

V. CONCLUSION

This study presents an Enhanced Energy Prediction framework for next-generation urban buildings using a Pyramidal Dilation Attention Convolutional Deep Neural Network optimized with Bitterling Fish Optimization (EEP-UB-PDACN-BFO). Input data were sourced from the Building Energy Ratings (BER) dataset, and the Pyramidal Dilation Attention Convolutional Network (PDACN) was employed to forecast Energy Use Intensity (EUI).

Compared to existing methods, including the Gradient Boosting Algorithm (UBEPP-RAD-GBA), the Time Series Forecasting for Urban Building Energy Consumption according to Graph Convolutional Network (TSF-UBEC-DCN), and the Multi-objective Optimization of Building Energy Performance and Indoor Thermal Comfort by Combining Artificial Neural Networks and Metaheuristic Algorithms (BEP-ITC-ANN), the proposed model delivered superior performance, achieving the lowest Root Mean Square Error (RMSE) of 6.2 kWh/(m^2·year), the highest R^2 score of 0.95, the lowest Mean Absolute Error (MAE) of 3.9 kWh/(m^2·year), the lowest Mean Squared Error (MSE) of 0.0750 √(kWh/(m^2·year)), and the lowest Mean Absolute Percentage Error (MAPE) of 0.45%. These results establish the EEP-UB-PDACN-BFO framework as a highly effective tool for accurate energy prediction in urban buildings.

Future work should investigate the influence of various non-residential archetypes, mid-rise, and high-rise apartment buildings on the predictive capability of machine learning models. Additionally, integrating parametric modelling within cloud computing platforms may further enhance performance. While this study focuses on annual energy consumption, extending the analysis to monthly and seasonal variations would offer deeper insights into energy performance trends.

ACKNOWLEDGMENT

The authors gratefully acknowledge Prince Sattam bin Abdulaziz University for funding this research under project number (PSAU/2024/01/31833).

REFERENCES

[1] U. Perwez, Y. Yamaguchi, T. Ma, Y. Dai, and Y. Shimoda, "Multi-scale GIS-synthetic hybrid approach for the development of commercial building stock energy model," *Applied Energy*, vol. 323, Oct. 2022, Art. no. 119536, https://doi.org/10.1016/j.apenergy.2022.119536.

[2] F. Johari, F. Shadram, and J. Widén, "Urban building energy modeling from geo-referenced energy performance certificate data: Development, calibration, and validation," *Sustainable Cities and Society*, vol. 96, Sep. 2023, Art. no. 104664, https://doi.org/10.1016/j.scs.2023.104664.

[3] A. Malhotra, M. Shamovich, J. Frisch, and C. Van Treeck, "Urban energy simulations using open CityGML models: A comparative analysis," *Energy and Buildings*, vol. 255, Jan. 2022, Art. no. 111658, https://doi.org/10.1016/j.enbuild.2021.111658.

[4] U. Ali *et al.*, "Urban building energy performance prediction and retrofit analysis using data-driven machine learning approach," *Energy and Buildings*, vol. 303, Jan. 2024, Art. no. 113768, https://doi.org/10.1016/j.enbuild.2023.113768.

[5] S. Wenninger, C. Kaymakci, and C. Wiethe, "Explainable long-term building energy consumption prediction using QLattice," *Applied Energy*, vol. 308, Feb. 2022, Art. no. 118300, https://doi.org/10.1016/j.apenergy.2021.118300.

[6] M. S. Geraldi and E. Ghisi, "Data-driven framework towards realistic bottom-up energy benchmarking using an Artificial Neural Network," *Applied Energy*, vol. 306, Jan. 2022, Art. no. 117960, https://doi.org/10.1016/j.apenergy.2021.117960.

[7] J. Lizana, V. P. López-Cabeza, R. Renaldi, E. Diz-Mellado, C. Rivera-Gómez, and C. Galán-Marín, "Integrating courtyard microclimate in building performance to mitigate extreme urban heat impacts," *Sustainable Cities and Society*, vol. 78, Mar. 2022, Art. no. 103590, https://doi.org/10.1016/j.scs.2021.103590.

[8] A. Nakhaee and A. Paydar, "DeepRadiation: An intelligent augmented reality platform for predicting urban energy performance just through 360 panoramic streetscape images utilizing various deep learning models," *Building Simulation*, vol. 16, no. 3, pp. 499–510, Mar. 2023, https://doi.org/10.1007/s12273-022-0953-5.

[9] Y. Zhang, A. Schlueter, and C. Waibel, "SolarGAN: Synthetic annual solar irradiance time series on urban building facades via Deep Generative Networks," *Energy and AI*, vol. 12, Apr. 2023, Art. no. 100223, https://doi.org/10.1016/j.egyai.2022.100223.

[10] X. Jin, F. Xiao, C. Zhang, and A. Li, "GEIN: An interpretable benchmarking framework towards all building types based on machine learning," *Energy and Buildings*, vol. 260, Apr. 2022, Art. no. 111909, https://doi.org/10.1016/j.enbuild.2022.111909.

[11] A. Soni, R. Koner, and V. G. K. Villuri, "Fusion of Dual-Scale Convolution Neural Network for Urban Building Footprints," *Ain Shams Engineering Journal*, vol. 13, no. 3, May 2022, Art. no. 101622, https://doi.org/10.1016/j.asej.2021.10.017.

[12] D. Shi, Y. Gao, P. Zeng, B. Li, P. Shen, and C. Zhuang, "Climate adaptive optimization of green roofs and natural night ventilation for lifespan energy performance improvement in office buildings," *Building and Environment*, vol. 223, Sep. 2022, Art. no. 109505, https://doi.org/10.1016/j.buildenv.2022.109505.

[13] P. Lin, L. Zhang, and J. Zuo, "Data-driven prediction of building energy consumption using an adaptive multi-model fusion approach," *Applied Soft Computing*, vol. 129, Nov. 2022, Art. no. 109616, https://doi.org/10.1016/j.asoc.2022.109616.

[14] S. Han, H. Shao, Z. Huo, X. Yang, and J. Cheng, "End-to-end chiller fault diagnosis using fused attention mechanism and dynamic cross-entropy under imbalanced datasets," *Building and Environment*, vol. 212, Mar. 2022, Art. no. 108821, https://doi.org/10.1016/j.buildenv.2022.108821.

[15] Z. Deng, K. Javanroodi, V. M. Nik, and Y. Chen, "Using urban building energy modeling to quantify the energy performance of residential buildings under climate change," *Building Simulation*, vol. 16, no. 9, pp. 1629–1643, Sep. 2023, https://doi.org/10.1007/s12273-023-1032-2.

[16] J. An, Y. Wu, C. Gui, and D. Yan, "Chinese prototype building models for simulating the energy performance of the nationwide building stock," *Building Simulation*, vol. 16, no. 8, pp. 1559–1582, Aug. 2023, https://doi.org/10.1007/s12273-023-1058-5.

[17] Z. Jalali, A. Y. Shamseldin, and A. Ghaffarianhoseini, "Urban microclimate impacts on residential building energy demand in Auckland, New Zealand: A climate change perspective," *Urban Climate*, vol. 53, Jan. 2024, Art. no. 101808, https://doi.org/10.1016/j.uclim.2024.101808.

[18] F. Battini, G. Pernigotto, and A. Gasparella, "District-level validation of a shoeboxing simplification algorithm to speed-up Urban Building Energy Modeling simulations," *Applied Energy*, vol. 349, Nov. 2023, Art. no. 121570, https://doi.org/10.1016/j.apenergy.2023.121570.

[19] F. E. Sapnken, M. M. Hamed, B. Soldo, and J. Gaston Tamba, "Modeling energy-efficient building loads using machine-learning algorithms for the design phase," *Energy and Buildings*, vol. 283, Mar. 2023, Art. no. 112807, https://doi.org/10.1016/j.enbuild.2023.112807.

[20] U. Perwez, K. Shono, Y. Yamaguchi, and Y. Shimoda, "Multi-scale UBEM-BIPV coupled approach for the assessment of carbon neutrality of commercial building stock," *Energy and Buildings*, vol. 291, Jul. 2023, Art. no. 113086, https://doi.org/10.1016/j.enbuild.2023.113086.

[21] P. Sutthichaimethee, W. Sa-Ngiamvibool, B. Wattana, J. Luo, and S. Wattana, "A Long-Term Electricity Consumption Model adapted from the MMM-ARCH-M Framework for Strategic Greenhouse Gas Emission Reduction towards Smart City Goals in Thailand," *Engineering, Technology & Applied Science Research*, vol. 15, no. 3, pp. 22367–22377, Jun. 2025, https://doi.org/10.48084/etasr.10363.

[22] *Irish Building Energy Ratings (BER) Dataset*. (2023), J. McNeill. [Online]. Available: https://www.kaggle.com/datasets/datajmcn/berpublicdata.

[23] J. Nako, C. Psychalinos, F. Khateb, and A. S. Elwakil, "Bilinear Double-Order Filter Designs and Application Examples," *IEEE Access*, vol. 12, pp. 14040–14049, 2024, https://doi.org/10.1109/ACCESS.2024.3357092.

[24] W. Hou, N. Chen, J. Peng, W. Sun, and Q. Du, "Pyramidal Dilation Attention Convolutional Network With Active and Self-Paced Learning for Hyperspectral Image Classification," *IEEE Journal of Selected Topics in Applied Earth Observations and Remote Sensing*, vol. 16, pp. 1503–1518, 2023, https://doi.org/10.1109/JSTARS.2023.3237566.

[25] L. Zareian, J. Rahebi, and M. J. Shayegan, "Bitterling fish optimization (BFO) algorithm," *Multimedia Tools and Applications*, vol. 83, no. 31, pp. 75893–75926, Feb. 2024, https://doi.org/10.1007/s11042-024-18579-0.

[26] K. Elhabyb, A. Baina, M. Bellafkih, and A. F. Deifalla, "Machine Learning Algorithms for Predicting Energy Consumption in Educational Buildings," *International Journal of Energy Research*, vol. 2024, no. 1, Jan. 2024, Art. no. 6812425, https://doi.org/10.1155/2024/6812425.

[27] H. B. Juričić and H. Krstić, "Comparing MLR and ANN models for school building electrical energy prediction in Osijek-Baranja County in Croatia," *Energy Reports*, vol. 12, pp. 3595–3606, Dec. 2024, https://doi.org/10.1016/j.egyr.2024.09.039.

[28] Y. Shen *et al.*, "Utilizing interpretable stacking ensemble learning and NSGA-III for the prediction and optimisation of building photo-thermal environment and energy consumption," *Building Simulation*, vol. 17, no. 5, pp. 819–838, May 2024, https://doi.org/10.1007/s12273-024-1108-7.

AUTHORS PROFILE

Dr. Suleman Alnatheer is an Assistant Professor in Computer Engineering at Prince Sattam bin Abdulaziz University. His research focuses on statistical learning theory and its applications in next-generation wireless communication technologies. He teaches undergraduate courses in various electrical and computer engineering subjects. Prior to joining Prince Sattam bin Abdulaziz University, Dr. Alnatheer served as a lecturer at the College of Telecommunication and Information, where he collaborated with

distinguished colleagues. He holds a Ph.D. from Stevens Institute of Technology, and an M.Sc. and B.Sc. from George Washington University.

Dr. Mohammed Altaf Ahmed received his Ph.D. in Electronics & Communication Engineering from GITAM University, Vishakhapatnam, India, in 2018, earning the Best Thesis Award and a Gold Medal. He completed his M.Eng. in Embedded Systems from Jawaharlal Nehru Technological University, Hyderabad, India, in 2008, and his B.Eng. in Electronics and Communications from Swami Ramanand Teerth Marathwada University, Nanded, India, in 2000. His current research focuses on VLSI design, embedded systems, artificial intelligence, and IoT devices. Dr. Ahmed has successfully executed several research projects in these areas and has published extensively in leading peer-reviewed journals indexed in Scopus and Science Citation Index.